

## LOCAL DIFFERENCES IN MYOTENDINOUS JUNCTIONS IN AXIAL MUSCLE FIBRES OF CARP (*CYPRINUS CARPIO* L.)

IGOR L. Y. SPIERTS, H. A. AKSTER, I. H. C. VOS AND J. W. M. OSSE

Department of Experimental Animal Morphology and Cell Biology, Agricultural University, Marijkeweg 40,  
NL-6709 PG Wageningen, The Netherlands

Accepted 6 December 1995

### Summary

We studied the myotendinous junctions of anterior and posterior red and white axial muscle fibres of carp using stereology. In posterior axial muscle fibres of swimming fish, stress (load on the myotendinous junction) must be higher than in anterior fibres as posterior fibres have a longer phase of eccentric activity. As we expected the magnitude of the load on the junction to be reflected in its structure, we compared the interfacial ratio, the ratio between the area of the junctional sarcolemma and the cross-sectional fibre area, of these muscle fibres. This ratio

differed significantly between the investigated groups, with red fibres and posterior fibres having the larger ratios. The higher interfacial ratio of posterior myotendinous junctions is in accordance with the proposition mentioned above. The difference between myotendinous junctions of red and white fibres is probably related to a difference in the duration of the load on the junction.

Key words: carp, *Cyprinus carpio*, muscle fibre types, myotendinous junction, force transmission, fish swimming.

### Introduction

At the myotendinous junction (MTJ), forces generated or transmitted by the myofibrils are transferred to the collagen fibres of the tendon. The muscle fibre and the tendon interdigitate, which results in an amplification of the interfacial membrane area and in a reduction in local stress (force per unit area). The interdigitation of muscle and tendon also results in a shift from tensile load to shear load. The angle  $\alpha$  between the muscle fibre membrane and the direction of the force applied to the joint (transmitted by the actin filaments) is indicative of the amount of shear loading; a smaller value of  $\alpha$  indicates more loading in shear (Lubkin, 1957; Tidball, 1983). Joints loaded in shear are commonly found to be much stronger than those loaded in tension (Bikerman, 1968) and a smaller value of  $\alpha$  is assumed to result in a stronger MTJ (Tidball, 1983; Tidball and Daniel, 1986). The magnitude of the load on the MTJ is expected to influence the amplification of the interfacial membrane area and angle  $\alpha$ . Decrease of the load on the muscle, caused by disuse (Tidball, 1983; Kannus *et al.* 1992) or by space-flight (Tidball and Quan, 1992), indeed resulted in an increase in the values of  $\alpha$  (Tidball, 1983) or in a decrease in the membrane amplification (Tidball and Quan, 1992; Kannus *et al.* 1992). Tidball and Daniel (1986) considered that the duration of the load may also significantly influence the demands imposed upon the junction. This assumption is based on the viscoelastic properties of the junction and the fluid nature of the membrane.

Membrane amplification at the MTJ showed no consistent

relationship to 'muscle fibre type characteristics' (tonic *versus* phasic and slow twitch *versus* fast twitch; Trotter *et al.* 1985a,b; Tidball and Daniel, 1986; Trotter and Baca, 1987; Kannus *et al.* 1992; Trotter, 1993). However, 'fibre type' denotes a combination of muscle fibre properties, and fibres of the same type may differ in the type of activity (see below). *In vitro*, most muscles experience cyclic alternations of contraction and lengthening. Tension development (loading of the MTJ) depends on  $V/V_{\max}$ , the ratio between the actual contraction velocity and the maximal (unloaded) contraction velocity of the fibre (Hill, 1938), and eccentric activity (negative contraction velocity) results in tensions higher than those during concentric activity.

Axial muscles of fish contain spatially separated muscle zones that differ in activity pattern. A laterally situated strip of red muscle is used for slow continuous activity. The bulk of the musculature, which consists of white muscle fibres, is used for short powerful bursts of activity (Hudson, 1973; Johnston *et al.* 1974, 1975; Akster and Osse, 1978; Bone, 1978; Proctor *et al.* 1980; Rome *et al.* 1988; Altringham and Johnston, 1990a,b; van Leeuwen *et al.* 1990).

In addition to the medial-lateral difference in fibre types, there are also antero-posterior differences in muscle function between fibres of the same type in the body of a swimming fish. Computer models (van Leeuwen *et al.* 1990; van Leeuwen, 1995) based on electromyographic and motion analysis of carp (*Cyprinus carpio* L.) predicted that, during

continuous and intermittent swimming, muscle fibres in the tail region (together with the connective tissue) would play an important role in the transmission of force produced by more anterior muscle fibres. The posterior fibres have a longer phase of eccentric activity than the anterior fibres (van Leeuwen *et al.* 1990; van Leeuwen, 1995). As a result, these posterior fibres will develop greater forces than the anterior fibres. This expectation was confirmed by simulation experiments (Davies *et al.* 1995). We expect that greater forces in posterior fibres will be accompanied by a greater membrane amplification at the MTJ.

The MTJ of the common carp shows a general resemblance in morphology (Akster *et al.* 1995) to the MTJs previously characterized in a wide variety of vertebrates from hagfish to mammals, including teleosts (Hanak and Böck, 1971; Korneliussen, 1973; Schattenberg, 1973; Trotter *et al.* 1981, 1983a,b, 1985a,b; Trotter and Baca, 1987; Trotter, 1990, 1993; Tidball, 1983, 1984; Tidball and Daniel, 1986; Tidball and Quan, 1992; Ishikawa *et al.* 1983; Eisenberg and Milton, 1984; Bremner and Hallett, 1985; Hallett and Bremner, 1988).

In this study we have investigated the MTJs of both anterior and posterior axial white and red muscle fibres of the common carp, by means of stereology (Eisenberg and Milton, 1984), to determine whether the published differences in loading of these fibres are accompanied by differences in the structure of the MTJ.

### Materials and methods

Three common carp (*Cyprinus carpio* L.) of 19–24 cm standard length, bred in the laboratory at 23 °C, and fed on commercial fish food (trouvut pellets; Trouw and Co. Putten), were used.

The fish were killed with an overdose (0.2 %) of tricaine methane sulphonate (Sandoz). A piece of skin was removed and Karnovsky's fixative (Karnovsky, 1965) was injected into the axial muscle. After fixation *in situ* at room temperature for about 15 min, small pieces of red and white axial muscle (approximately 10 mm × 5 mm × 3 mm) were dissected from the tail region near the anus (posterior) and from the body region immediately rostral to the fourth ray of the dorsal fin (anterior, Fig. 1). When superficial white axial muscle was dissected, care was taken to avoid red and pink muscle layers. Fixation was continued for approximately 90 min in fresh Karnovsky's fixative. The muscle tissue was rinsed in 0.1 % cacodylate buffer, pH 7.3.

MTJs were prepared for scanning electron microscopy as described by Trotter and Baca (1987). For transmission electron microscopy, the muscle tissue was postfixed in 1 % osmium tetroxide, followed by 1 % uranyl acetate, dehydrated in graded alcohols and propylene oxide, and embedded in an epon mixture.

### Sampling procedure

Four sample sites (anterior and posterior red and anterior and posterior white) and six fibres per sample site were examined

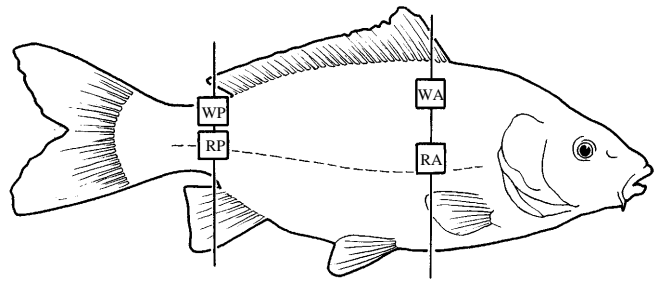


Fig. 1. Position of the muscle sample sites on the common carp *Cyprinus carpio*, indicated by rectangles. W, white muscle; R, red muscle; A, anterior; P, posterior.

for each of the three fish. Two or three blocks of tissue were taken from each sampling site. Ultrathin longitudinal sections were made from each block using a diamond knife on a Reichert-Jung Ultracut E ultramicrotome. The ultrathin sections were stained with uranyl acetate and lead citrate.

Owing to the orientation of axial muscle fibres of fish in oblique fibre trajectories (Alexander, 1969), slight differences in the direction of the muscle fibres occur at the sample sites. Transmission electron micrographs were made of the MTJs of the first two (or three, depending on the number of blocks obtained from the sample site) truly longitudinally sectioned fibres that were identified under a Philips EM 201C electron microscope. Sections were considered to be longitudinal when thick filaments could be traced over the entire length of an A-band. Deformation by fixation was considered to be minimal when the angle between the filaments and the Z-line was approximately 90°. The beginning of the MTJ was defined as the middle of the location where the membrane on both sides of the fibre profile was not parallel for at least two sarcomere lengths.

For random morphometric sampling, the micrograph area, indicated on the image screen of the microscope, was used as a sample area. A micrograph (×25 500) was made of every fourth area of the interfascial membrane and used for subsequent morphometric analysis. For each fibre, the starting point for sampling was obtained using a sampling scheme containing twelve different starting points (the first, second, third and fourth frames from the left side, the right side and the middle of the MTJ of the fibre). This resulted in 3–5 micrographs per fibre and about 24 micrographs per sample site from each fish.

Lower-magnification micrographs (×2400) of every fibre were used to measure the diameter of the fibre profile,  $d_f$ , and the length of the MTJ ( $L_{mtj}$ , the distance between the last Z-line before the beginning of the taper and the tip of the taper). The diameter of the fibre profile was measured at a location where the membrane on both sides of the fibre profile was parallel.

### Morphometry

Sectioning muscle fibres with a diameter  $D_f$  produces a population of fibre profiles with a mean diameter  $\bar{d}_f$ . Only a

small part of the profile is cut through the real diameter,  $D_f$ . The mean fibre diameter,  $\bar{d}_f$ , measured from the electron micrographs, is an undervaluation of the real fibre diameter,  $D_f$ . For circular fibres, randomly sampled in longitudinal sections, the real fibre diameter can be calculated (Weibel and Bolender, 1973) by:

$$D_f = (4/\pi)\bar{d}_f. \quad (1)$$

Amplification of the membrane area at MTJs is defined as the interfacial ratio (IFR), the ratio of the interfacial membrane area ( $S_m$ ) to the cross-sectional area of the fibre ( $S_c$ ), where:

$$\text{IFR} = S_m/S_c. \quad (2)$$

This ratio was calculated using stereological methods (Merz, 1967; Weibel and Bolender, 1973; Aherne and Dunnill, 1982; Royet, 1991) with a 2 cm semicircular test grid placed on the micrograph. The method was adjusted for muscle fibres by Eisenberg and Milton (1984). The membrane area per unit volume ( $S_m/V$ ) was calculated from the number of intersections ( $I_m$ ) between the interfacial membrane of the fibre and the test grid. The fibre cross-sectional area was obtained from the projected length of the interfacial membrane on the plane of the last Z-disc before the beginning of the taper (Tidball, 1983). The cross-sectional area per unit volume ( $S_c/V$ ) was calculated from the number of intersections ( $I_c$ ) between this projection and the test grid.

Muscle is highly anisotropic, it has a high degree of orientation. This means that projections of the membrane on a plane perpendicular to the fibre axis and on a plane parallel to the fibre axis are not equal (as they would be in a purely isotropic system). DeHoff and Rhines (1968) called this type of anisotropy linear. For every specific geometry with a known degree of orientation, an appropriate constant is necessary to relate the boundary length seen in the micrographs to a surface area in the real tissue. Some specific constants have been derived and are reviewed by Eisenberg (1983).

The stereological equations relating the area of interfacial membrane per unit volume ( $S_m/V$ ) to the number of intersections between the membrane and the line length of the test grid ( $I_m/L$ ) for an isotropic orientation of the membrane are (Eisenberg, 1983):

$$S_{\text{isotropic}}/V = 2I_m/L, \quad (3)$$

and for an anisotropic orientation of the membrane:

$$S_{\text{anisotropic}}/V = (\pi^2/4)I_m/L. \quad (4)$$

For the fibre cross section, the equation is:

$$S_c/V = (\pi/2)I_c/L. \quad (5)$$

The percentage anisotropy (% anisotropy) of the interfacial membrane was determined in every second fibre from the number of intersections with the parallel ( $I_{\parallel}$ ) and perpendicular ( $I_{\perp}$ ) lines of a 1 cm  $\times$  1 cm test grid. Orientation of the grid lines was parallel and perpendicular to the fibre axis. According to

DeHoff and Rhines (1968) and to Eisenberg and Milton (1984):

$$\% \text{anisotropy} = 100(I_{\perp} - I_{\parallel})/(0.273I_{\parallel} + I_{\perp}). \quad (6)$$

Using equations 2–6, and  $f_{\text{isotr}}$  and  $f_{\text{anisotr}}$  for, respectively, the fractional isotropy and anisotropy of the membrane, the IFR is given by:

$$\text{IFR} = \frac{[2f_{\text{isotr}} + (\pi^2/4)f_{\text{anisotr}}]I_m}{(\pi/2)I_c}. \quad (7)$$

We determined two IFR values,  $\text{IFR}_{\text{em}}$  (entire membrane IFR) and  $\text{IFR}_{\text{am}}$  (attachment membrane IFR). For  $\text{IFR}_{\text{em}}$ , the surface of the entire interfacial membrane ( $S_{\text{em}}$ ) was considered. Only caveolae were excluded; they were treated as if the membrane continued over their mouth without interruption. For  $\text{IFR}_{\text{am}}$ , only that part of the surface of the membrane where actin filaments attached to the membrane ( $S_{\text{am}}$ ) was considered. The presence of actin filaments along the membrane or a thickened cell membrane (a clearly visible lamina densa and a thick glycocalyx with a descending gradient in the direction of the lamina densa) were the criteria used to assess this portion of the interfacial membrane. In case of doubt, the cell membrane was always considered to be attachment membrane.

#### Statistics

All data measured in this study appeared to be normally distributed (Shapiro and Wilk, 1965). Statistical analyses of the measured differences in  $L_{\text{mtj}}$ ,  $D_f$ ,  $\text{IFR}_{\text{em}}$  and  $\text{IFR}_{\text{am}}$  were performed using analysis of variance (ANOVA). Statements of statistical significance are based on  $P \leq 0.05$ , unless specified otherwise (Sokal and Rohlf, 1981; Rohlf and Sokal, 1981).

## Results

### Shape of the MTJs

Red and white fibres differ in the type of membrane folding at the MTJ. Red fibres attach mainly perpendicular to the fascial plane of the tendon (myosept) and their MTJs have large finger-like extensions (Figs 2, 3). White fibres attach at an angle to the fascial plane of the tendon and their MTJs have more, but smaller, finger-like extensions (Figs 4–6).

White fibres have a significantly larger mean fibre diameter ( $44.58 \pm 13.74 \mu\text{m}$ ) than red fibres ( $32.38 \pm 10.62 \mu\text{m}$ ,  $P=0.0001$ ) and posterior fibres have a significantly larger mean fibre diameter ( $41.29 \pm 12.28 \mu\text{m}$ ) than anterior fibres ( $35.67 \pm 14.47 \mu\text{m}$ ,  $P=0.045$ ) (Table 1). These values are corrected for the underestimation caused by measuring diameter profiles in thin sections (see Materials and methods), but not for shrinkage.  $L_{\text{mtj}}$ , the length of the tapering fibre end, is significantly greater in white than in red fibres (Table 1).  $L_{\text{mtj}}$  is not corrected for the underestimation caused by measuring this variable from thin sections through a tapering fibre end, so that values including this variable are relative, not absolute.  $L_{\text{mtj}}$  divided by  $D_f$  gives a rough impression of the general shape of the fibre end (Table 1). This ratio is not significantly

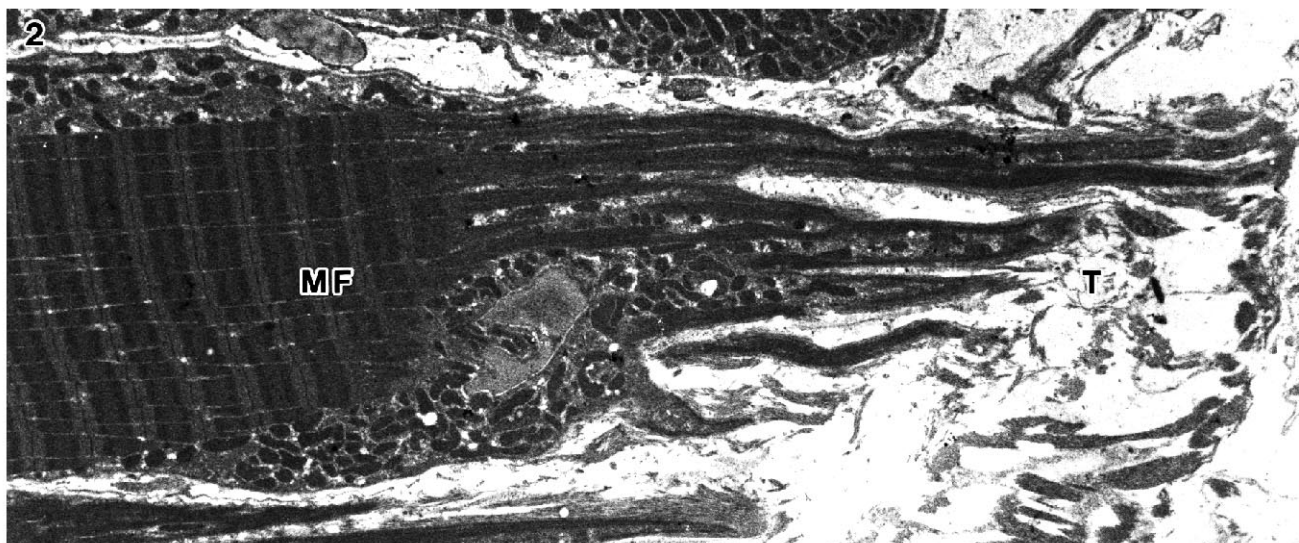


Fig. 2. Transmission electron micrograph of a longitudinally sectioned myotendinous junction (MTJ) of a red axial muscle fibre. Long bundles of actin filaments connect the myofibrils (MF) with the interfascial membrane. Long finger-like protrusions extend into the tendon (T).  $\times 2400$ .

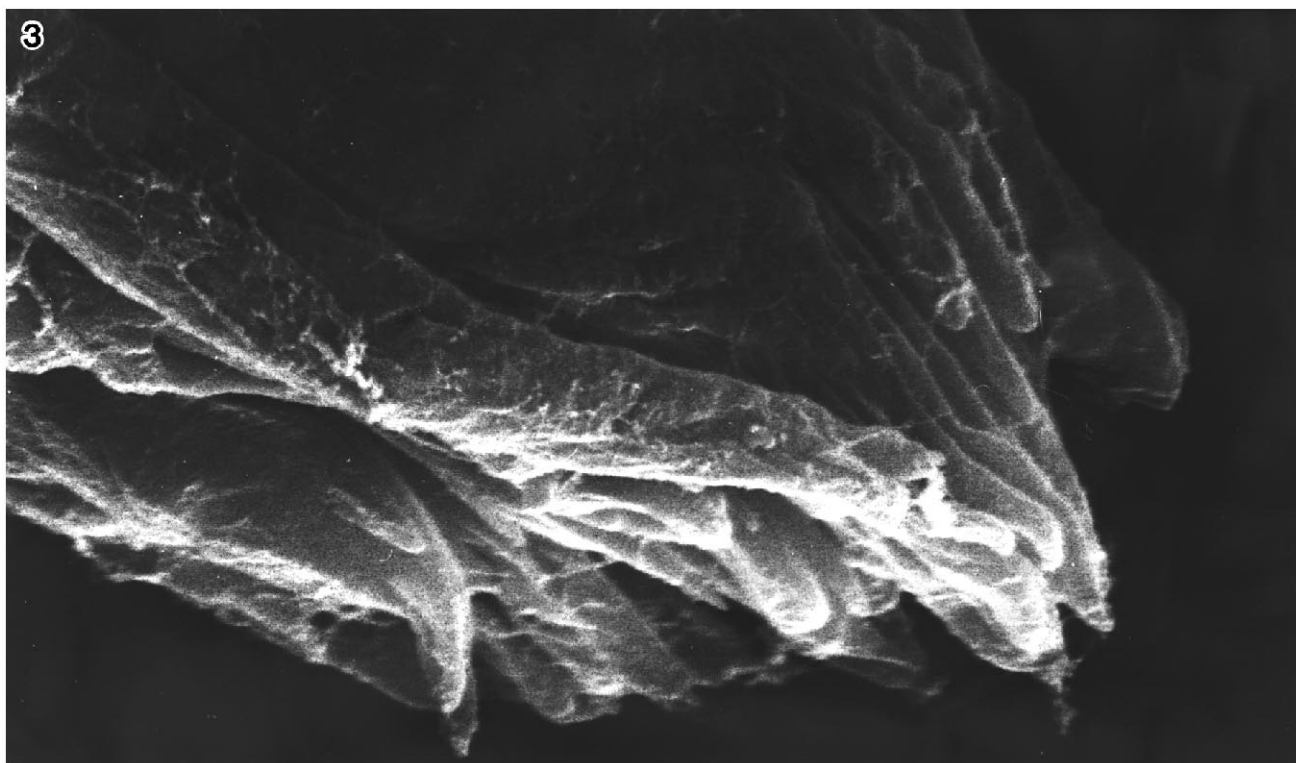


Fig. 3. Scanning electron micrograph of a red axial muscle fibre. Note the large finger-like extensions.  $\times 7300$ .

different between anterior and posterior fibres, indicating that the general shape of the MTJ anteriorly and posteriorly is comparable. White fibre MTJs are thick-set ( $L_{mtj}/D_f = 1.07 \pm 0.17$ ) compared with the more slender red fibre MTJs ( $L_{mtj}/D_f = 1.32 \pm 0.31$ ,  $P = 0.0001$ ).

#### *Stereological analysis of the MTJs*

IFR<sub>em</sub> (entire membrane IFR) and IFR<sub>am</sub> (attachment

membrane IFR), were calculated by means of morphometry. No significant differences between individual fish were found on the IFR values. The values for IFR<sub>am</sub> are consistently 85–90% of the values for the corresponding IFR<sub>em</sub> (Table 2). IFR<sub>em</sub> and IFR<sub>am</sub> show similar significant differences for muscle type, muscle location and combined effects; therefore, we will limit the description to IFR<sub>em</sub>.

The muscle type effect is very large ( $P = 0.0001$ ). For red

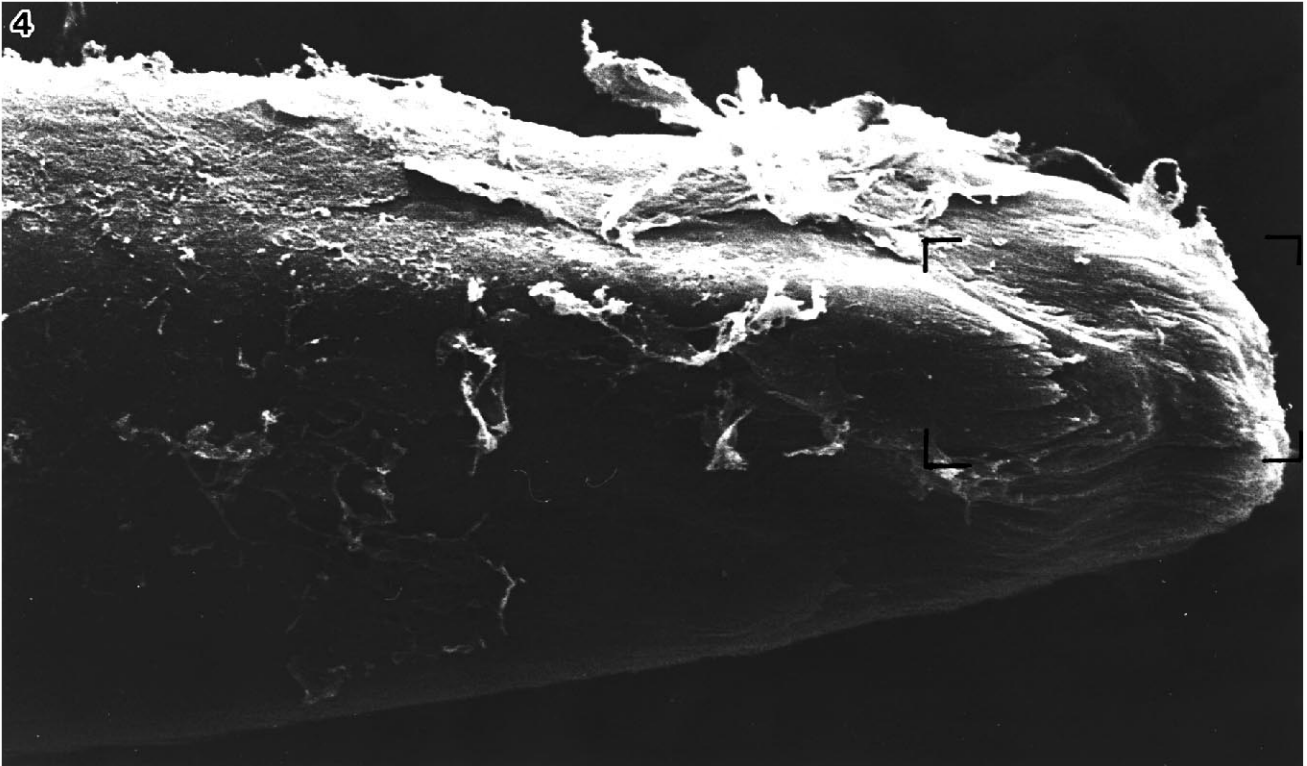


Fig. 4. Scanning electron micrograph of a white axial muscle fibre. The asymmetrical taper indicates that the fibre attaches at an angle to the fascial plane of the tendon.  $\times 2100$ . The marked area is also shown in Fig. 5.

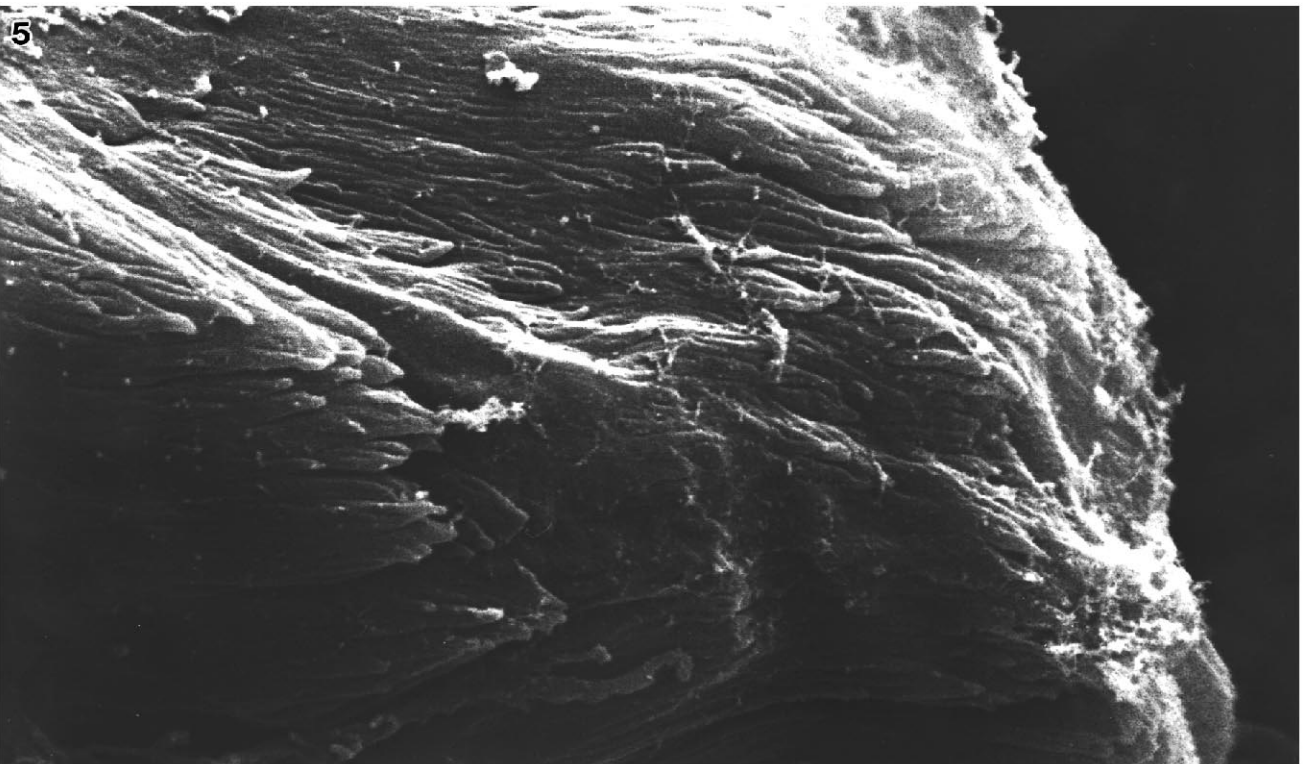


Fig. 5. Detail of Fig. 4 at the same magnification ( $\times 7300$ ) as that of the red axial muscle fibre in Fig. 3. The finger-like extensions of the white fibre are smaller and more numerous than those of the red fibre.

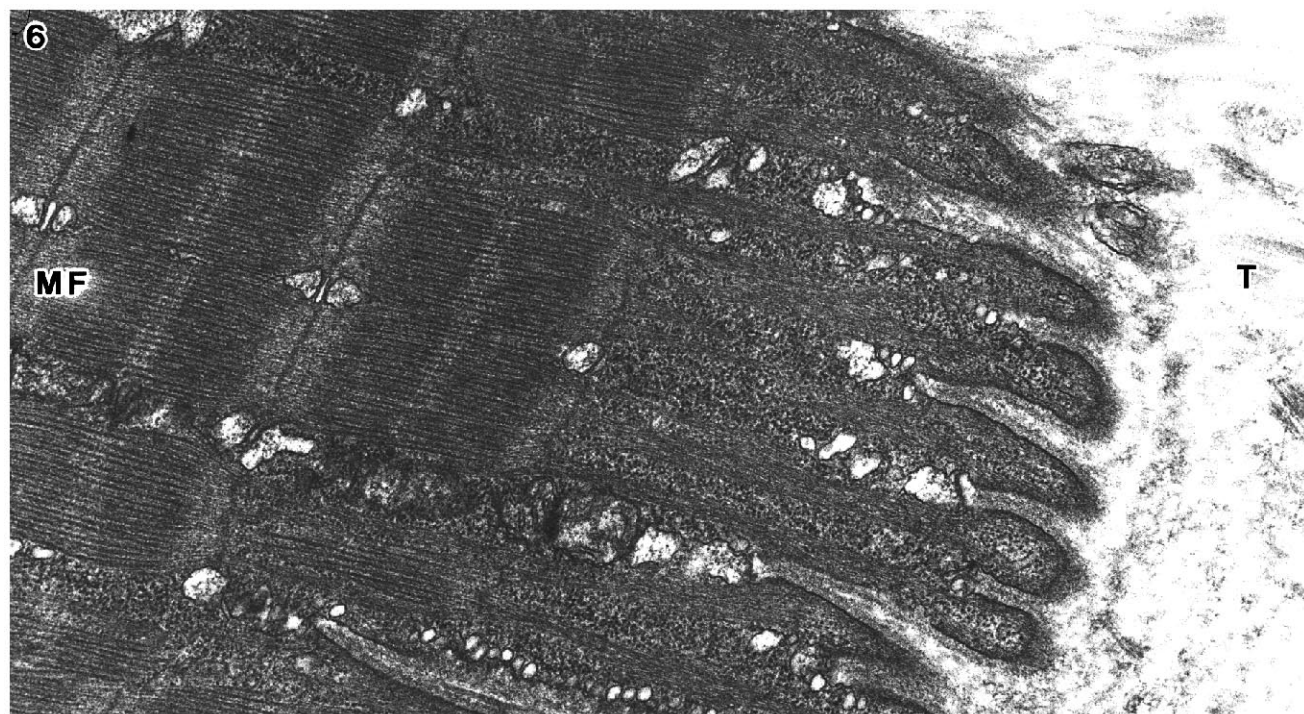


Fig. 6. Transmission electron micrograph of a longitudinally sectioned myotendinous junction (MTJ) of a white axial muscle fibre. Note the shallow finger-like extensions. MF, myofibrils; T, tendon.  $\times 18\,500$ .

Table 1. *Morphometric values of the myotendinous junctions*

Type	Fibre diameter, $D_f$ ( $\mu\text{m}$ )	Length of MTJ, $L_{\text{mtj}}$ ( $\mu\text{m}$ )	$L_{\text{mtj}}/D_f$
Red, anterior ( $N=18$ )	$30.10\pm 10.63^a$	$38.63\pm 10.17^a$	$1.35\pm 0.29^a$
Red, posterior ( $N=18$ )	$34.66\pm 10.10^{a,b}$	$42.32\pm 6.64^{a,b}$	$1.30\pm 0.32^a$
White, anterior ( $N=18$ )	$41.25\pm 15.61^{b,c}$	$45.32\pm 15.73^{a,b}$	$1.13\pm 0.17^b$
White, posterior ( $N=18$ )	$47.92\pm 10.56^c$	$48.88\pm 13.06^b$	$1.02\pm 0.15^b$
Anterior, total ( $N=36$ )	$35.67\pm 14.47^a$	$41.98\pm 13.66^a$	$1.24\pm 0.26^a$
Posterior, total ( $N=36$ )	$41.29\pm 12.28^b$	$45.60\pm 10.87^a$	$1.16\pm 0.28^a$
Red, total ( $N=36$ )	$32.38\pm 10.62^a$	$40.47\pm 8.79^a$	$1.32\pm 0.31^a$
White, total ( $N=36$ )	$44.58\pm 13.74^b$	$47.10\pm 14.57^b$	$1.07\pm 0.17^b$

Within each section of a column (mutually distinguished by blank lines), groups indicated with different letters (a,b,c) differ significantly ( $P\leq 0.05$ );  $N$ , number of fibres measured.  
Values are mean  $\pm$  S.D.  
MTJ, myotendinous junction.

muscle fibres (36 fibres), the mean  $\text{IFR}_{\text{em}}$  is  $8.20\pm 1.71$ ; for white fibres (36 fibres), it is  $6.29\pm 1.34$ . A significant difference in  $\text{IFR}_{\text{em}}$  was also found between posteriorly ( $7.76\pm 1.77$ , 36

fibres) and anteriorly ( $6.73\pm 1.68$ , 36 fibres) situated fibres ( $P=0.0048$ ). The combined effects of muscle type and muscle location led to the following set of declining mean  $\text{IFR}_{\text{em}}$  values (18 fibres): red posterior,  $8.77\pm 1.70$ ; red anterior,  $7.63\pm 1.63$ ; white posterior,  $6.75\pm 1.24$  and white anterior,  $5.83\pm 1.34$  (Table 2).  
The percentage of membrane area in the MTJ with an anisotropic orientation was significantly higher in red muscle tissue ( $68.19\pm 7.44\%$ , 18 fibres) than in white muscle tissue ( $63.66\pm 3.98\%$ , 18 fibres,  $P=0.021$ ). It did not differ significantly between posterior muscle tissue ( $66.42\pm 6.77\%$ , 18 fibres) and anterior muscle tissue ( $65.42\pm 5.92\%$ , 18 fibres).

Discussion

Shape of the MTJs

Red and white fibres differ in the angle of attachment to the tendon and in the general shape of the MTJ, expressed as the ratio  $L_{\text{mtj}}/D_f$ . These differences are in accordance with the difference in orientation of red and white axial muscle fibres of fish. White axial muscle fibres are situated in helical fibre trajectories, red fibres lie more parallel to the body axis (Alexander, 1969). In addition, there was an, as yet unexplained, difference in the size of the finger-like extensions (compare Figs 3 and 5). Red and white fibres also differ in the orientation of the interfacial membrane. The percentage of anisotropically orientated interfacial membrane in white fibres of carp (63.66 %) is close to the percentage of anisotropy found in white fibres of the sartorius muscle of the frog *Rana temporaria* (approximately 60%; Eisenberg and Milton,



Table 2. The calculated interfacial ratios of the myotendinous junctions and the percentages anisotropy of the muscle tissue

Type	Entire membrane IFR <sub>em</sub>	Attachment membrane IFR <sub>am</sub>	IFR <sub>am</sub> /IFR <sub>em</sub> (%)	Anisotropy of tissue (%)
Red, anterior (N=18)	7.63±1.63 <sup>a</sup>	6.77±1.50 <sup>a</sup>	88.87	64.89±8.32 <sup>a</sup>
Red, posterior (N=18)	8.77±1.70 <sup>b</sup>	7.93±1.75 <sup>b</sup>	90.42	71.49±5.54 <sup>b</sup>
White, anterior (N=18)	5.83±1.34 <sup>c</sup>	4.95±1.38 <sup>c</sup>	84.91	65.96±3.02 <sup>a</sup>
White, posterior (N=18)	6.75±1.24 <sup>a,c</sup>	5.92±1.18 <sup>a,c</sup>	87.70	61.35±3.81 <sup>a</sup>
Anterior, total (N=36)	6.73±1.68 <sup>a</sup>	5.7±1.65 <sup>a</sup>	84.47	65.42±5.92 <sup>a</sup>
Posterior, total (N=36)	7.76±1.77 <sup>b</sup>	6.92±1.77 <sup>b</sup>	89.18	66.42±6.77 <sup>a</sup>
Red, total (N=36)	8.20±1.71 <sup>a</sup>	7.35±1.77 <sup>a</sup>	89.63	68.19±7.44 <sup>a</sup>
White, total (N=36)	6.29±1.34 <sup>b</sup>	5.43±1.34 <sup>b</sup>	86.33	63.66±3.98 <sup>b</sup>

Within each section of a column (mutually distinguished by blank lines), groups indicated with different letters (a,b,c) differ significantly ( $P \leq 0.05$ ); N, number of fibres measured for calculating the interfacial ratios (IFRs); half of these amounts were used for calculating the percentage anisotropy.

Values are means  $\pm$  S.D.

1984). Red fibres have a higher percentage anisotropy (68.19%). The attachment of red fibres, which is almost perpendicular to the fascial plane of the tendon, and the greater slenderness of their junctions probably contribute to this higher anisotropy.

No significant differences in the ratio  $L_{mtj}/D_f$  were found between anterior and posterior fibres (Table 1).

#### Quantification procedure

The amplification of the membrane area was estimated using a stereological method (Weibel and Bolender, 1973; Weibel, 1979) that was adapted to the degree of anisotropy of the muscle tissue (Eisenberg and Milton, 1984). This method is reliable, efficient and precise compared with other methods (Weibel and Bolender, 1973; Royet, 1991) and it requires no presuppositions about the shape of the MTJ. This is important as red and white fibres differ in shape of the MTJ as well as in the angle of attachment of the fibres to the fascial plane of the tendon. Results obtained using this method are comparable with results obtained using other methods (Trotter, 1993).

We determined the IFR<sub>em</sub> (entire membrane IFR, without caveolae) and the IFR<sub>am</sub> (attachment membrane IFR) and obtained similar results for both. The IFR<sub>am</sub> values were 85–90% of the IFR<sub>em</sub> values for the different locations and muscle types, and for individual muscle fibres. This indicates that the criteria used to distinguish the attachment membrane were consistently applied. It also indicates that IFR<sub>em</sub> can be used as accurately as IFR<sub>am</sub>, which is more difficult to define, to compare amplifications of membrane areas.

We found that the membrane amplification at the MTJ differs significantly between anterior and posterior fibres and between red and white fibres; posterior fibres and red fibres having larger amplifications (Table 2).

#### Force transmission at the MTJs

According to the models of van Leeuwen *et al.* (1990) and van Leeuwen (1995), the posterior axial muscle fibres of carp experience a longer phase of eccentric activity than the more

anterior fibres, resulting in a negative contraction speed and work output and, hence, in larger forces in the posterior fibres. These predictions were corroborated by simulation experiments with cod *Gadus morhua*. When activation patterns and cycle frequencies, as observed *in vivo*, were imposed on isolated bundles of superficial cod white axial muscle fibres, posterior fibres developed higher forces than anterior fibres (Davies *et al.* 1995). Posterior muscle fibres are slower than anterior fibres (Rome *et al.* 1993; Altringham *et al.* 1993; Davies *et al.* 1995). Anterior and posterior fibres also differ in duty cycle (the proportion of the tail-beat cycle during which the muscle shows electromyographic activity), relaxation time and shortening inactivation time (Rome *et al.* 1993). But simulation experiments show that the resulting patterns of force duration are similar for anterior and posterior fibres (Rome *et al.* 1993; Altringham *et al.* 1993). Thus, the higher amplification of the membrane area in posterior fibres (Table 2) is indeed related to a larger load on the junction.

The difference in IFR between red and white fibres is less easily explained. Although in carp head muscle the measured maximal isometric stress is similar in red and white muscle, 120 kN m<sup>-2</sup> and 110 kN m<sup>-2</sup>, respectively (Granzier *et al.* 1983), in axial muscle it is smaller in red fibres than in white fibres (64 kN m<sup>-2</sup> and 209 kN m<sup>-2</sup>, respectively, at 23 °C; Johnston *et al.* 1985). As these values are not corrected for the differences in the volume percentages of connective tissue, capillaries and mitochondria between red and white muscle, the difference in net stress between red and white axial muscle must be smaller. However, it seems unlikely that net maximal isometric stress is higher in red fibres than in white fibres.

Other factors that can be expected to influence the structure of the MTJ are (1) a high contraction velocity, (2) a large strain and (3) a long duration of the load on the junction. Contraction velocity is lower in red fibres than in white fibres (Rome *et al.* 1988). Strain can reach high values in red fibres (Rome and Sosnicki, 1991), but such large strains occur at high tail-beat frequencies when red fibres have a high  $V/V_{max}$  ratio (Rome

and Sosnicki, 1991) and consequently a very low force production (van Leeuwen *et al.* 1990). Also, Tidball and Chan (1989) found in mechanical experiments on MTJs of single muscle fibres from frog (*Rana pipiens*) semitendinosus muscle that failure of the MTJ was independent of strain and of strain rate. Therefore, we do not expect the differences in IFR values found in this study to be related to differences in strain. It is more likely that the large strain fluctuations in red fibres (Rome and Sosnicki, 1991) will impose high demands on the series elastic elements (titin filaments, Wang *et al.* 1991) of these fibres. The third factor, the duration of the load on the junction, is longer in red than in white fibres; red fibres are active at lower tail-beat frequencies (longer cycle times) than white fibres and for longer periods. Tidball and Daniel (1986) proposed that the degree of membrane folding at the MTJ depends on the magnitude and on the duration of the load on the junction. Curtis (1961) and Rand (1964) have shown that the mechanical behaviour of cell membranes is dependent on loading time. At a certain shear load (caused by applying either a large load for a short time or a small load for a longer time), the behaviour of a cell membrane changes from elastic to viscous. This leads to a non-reversible structural rearrangement. The cell can survive such a load by reducing the stress on the membrane through an amplification of the membrane area. The greater IFR value of MTJs of red muscle fibres of the carp may be related to the longer duration of the load on the junction in this fibre type. As muscle fibres probably transmit part of the developed force by their lateral surface (Street, 1983; Trotter, 1993), it is also possible that this lateral transmission is more important in white than in red fibres. However, we have no observations that support this suggestion.

The IFR<sub>am</sub> values vary from approximately 5 (anterior white fibres) to approximately 8 (posterior red fibres). These values are lower than IFR values of mouse, chicken, snake and frog, summarized by Trotter (1993). The IFR<sub>am</sub> values for these species (also determined using the method of Eisenberg and Milton, 1984) are between approximately 9 (plantaris of adult mouse; Trotter and Baca, 1987) and 16 (sartorius of frog; Eisenberg and Milton, 1984). As far as we know, no other quantitative data reporting the amplification of the membrane area in fish have yet been published. Hallett and Bremner (1988) described the invaginations in MTJs of hoki (*Macruronus novaezelandiae*) as being shallow, which agrees with the low IFR values we found in carp.

The low IFR values in the MTJ of axial muscle of the carp suggest that, in these myomeric muscles, load on the MTJ is less intense or shorter-lasting than in the muscles that have been investigated in other vertebrates.

We thank Dr J. L. van Leeuwen for his valuable comment on the manuscript and Ms J. J. Taverne and Ms A. Clerx for skilled technical help with the electron microscopy. We also thank Mr. J. W. van de Wal for supplying the scanning electron micrographs and Mr W. A. Valen for help in preparing the illustrations.

## References

- AHERNE, W. A. AND DUNNILL, M. S. (1982). *Morphometry*. London: E. Arnold Ltd. 205pp.
- AKSTER, H. A. AND OSSE, J. W. M. (1978). Muscle fibres in head muscles of the perch *Percha fluviatilis* (L.), Teleostei. A histochemical and electromyographical study. *Neth. J. Zool.* **28**, 94–110.
- AKSTER, H. A., VAN DE WAL, J. W. AND VEENENDAAL, T. (1995). Interaction of force transmission and sarcomere assembly at the muscle–tendon junctions of carp (*Cyprinus carpio*): ultrastructure and distribution of titin (connectin) and  $\alpha$  actinin. *Cell. Tissue Res.* **281**, 517–524.
- ALEXANDER, R. MCN. (1969). The orientation of muscle fibres in the myomeres of fishes. *J. mar. biol. Ass.* **49**, 263–290.
- ALTRINGHAM, J. D. AND JOHNSTON, I. A. (1990a). Modelling muscle power output in a swimming fish. *J. exp. Biol.* **148**, 395–402.
- ALTRINGHAM, J. D. AND JOHNSTON, I. A. (1990b). Scaling effects in muscle function: power output of isolated fish muscle fibres performing oscillatory work. *J. exp. Biol.* **151**, 453–467.
- ALTRINGHAM, J. D., WARDLE, C. S. AND SMITH, C. I. (1993). Myotomal muscle function at different locations in the body of a swimming fish. *J. exp. Biol.* **182**, 191–206.
- BIKERMANN, J. J. (1968). Stresses in proper adhiants. In *The Science of Adhesive Joints*, 2nd edn, pp. 192–263. New York, London: Academic Press.
- BONE, Q. (1978). Locomotor muscle. In *Fish Physiology*, vol. VII (ed. W. S. Hoar and D. J. Randall), pp. 361–324. New York: Academic Press.
- BREMNER, H. A. AND HALLETT, I. C. (1985). Muscle fiber–connective tissue junctions in the fish blue grenadier (*Macruronus novaezelandiae*). A scanning electron microscopy study. *J. Food Sci.* **50**, 975–980.
- CURTIS, A. S. G. (1961). Timing mechanics in the specific adhesion of cells. *Exp. Cell Res.* **8**, S107–S122.
- DAVIES, L. F., JOHNSTON, I. A. AND VAN DE WAL, J. W. (1995). Muscle fibres in rostral and caudal myotomes of the Atlantic cod (*Gadus morhua* L.) have different mechanical properties. *Physiol. Zool.* **68**, 673–697.
- DEHOFF, R. T. AND RHINES, F. N. (1968). *Quantitative Microscopy*. New York: McGraw-Hill. 422pp.
- EISENBERG, B. R. (1983). Quantitative ultrastructure of mammalian skeletal muscle. In *Handbook of Physiology*, section 10 (ed. L. D. Peachey and R. H. Adrian), pp. 73–112. Bethesda, MD: American Physiological Society.
- EISENBERG, B. R. AND MILTON, R. L. (1984). Muscle fibre termination at the tendon in the frog's sartorius: A stereological study. *Am. J. Anat.* **171**, 273–284.
- GRANZIER, H. L. M., WIERSMA, J., AKSTER, H. A. AND OSSE, J. W. M. (1983). Contractile properties of a white- and a red-fibre type of the m. hyohyoideus of the carp (*Cyprinus carpio* L.). *J. comp. Physiol.* **149**, 441–449.
- HALLETT, I. C. AND BREMNER, H. A. (1988). Fine structure of the myocommata-muscle fibre junction in hoki (*Macruronus novaezelandiae*). *J. Sci. Food Agric.* **44**, 245–261.
- HANAK, H. AND BÖCK, P. (1971). Die Feinstruktur de Muskel-Sehnverbindung von Skelett- und Herzmuskel. *J. Ultrastruct. Res.* **36**, 68–85.
- HILL, A. V. (1938). The heat of shortening and the dynamic constants of muscle. *Proc. R. Soc. Lond. B* **126**, 136–195.
- HUDSON, R. C. L. (1973). On the function of the white muscles in



- teleosts at intermediate swimming speeds. *J. exp. Biol.* **58**, 509–522.
- ISHIKAWA, H., SAWADA, H. AND YAMADA, E. (1983). Surface and internal morphology of skeletal muscle. In *Handbook of Physiology* (ed. L. D. Peachey and R. H. Adrian), pp. 1–21. Bethesda, MD: American Physiological Society.
- JOHNSTON, I. A., PATTERSON, S., WARD, P. AND GOLDSPIK, G. (1974). The histochemical demonstration of microfibrillar adenosine triphosphatase activity in fish muscle. *Can. J. Zool.* **52**, 871–877.
- JOHNSTON, I. A., SIDELL, B. D. AND DRIEDZIC, W. R. (1985). Force–velocity characteristics and metabolism of carp muscle fibres following temperature acclimation. *J. exp. Biol.* **119**, 239–249.
- JOHNSTON, I. A., WARD, P. AND GOLDSPIK, G. (1975). Studies on the swimming musculature on the rainbow trout. I. Fibre types. *J. Fish Biol.* **7**, 451–458.
- KANNUS, P., JOZSA, L., KVIST, M., LEHTO, M. AND JÄRVINEN, M. (1992). The effect of immobilization on myotendinous junction: an ultrastructural, histochemical and immunohistochemical study. *Acta physiol. scand.* **144**, 387–394.
- KARNOVSKY, M. J. (1965). A formaldehyde glutaraldehyde fixative of high osmolality for use in electronmicroscopy. *J. Cell Biol.* **27**, 137A–138A.
- KORNELIUSSEN, H. (1973). Ultrastructure of myotendinous junctions in myxine and rat. Specializations between the plasma membrane and the lamina densa. *J. Anat. Entwickl. Gesch.* **142**, 91–101.
- LUBKIN, J. L. (1957). A theory of adhesive scarf joints. *J. appl. Mech.* **24**, 255–260.
- MERZ, W. A. (1967). Die Streckenmessung an gerichteten Strükturen im Mikroskop und ihre Anwendung zur Bestimmung ixon Oberflächen–Volumen-Relationen im Knochengewebe. *Mikroskope* **22**, 132.
- PROCTOR, C., MOSSE, P. R. L. AND HUDSON, R. C. L. (1980). A histochemical and ultrastructural study of the development of the propulsive musculature of the brown trout, *Salmo trutta* L., in relation to its swimming behaviour. *J. Fish Biol.* **16**, 309–329.
- RAND, R. P. (1964). Mechanical properties of the red cell membrane. II. Viscoelastic breakdown of the membrane. *Biophys. J.* **4**, 303.
- ROHLF, F. J. AND SOKAL, R. R. (1981). *Statistical Tables*, second edition. New York: W. H. Freeman and Company. 219pp.
- ROME, L. C., FUNKE, R. P., ALEXANDER, R. MCN., LUTZ, G., ALDRIDGE, H., SCOTT, F. AND FREADMAN, M. (1988). Why animals have different muscle fibre types. *Nature* **335**, 824–827.
- ROME, L. C. AND SOSNICKI, A. A. (1991). Myofilament overlap in swimming carp. II. Sarcomere length changes during swimming. *Am. J. Physiol.* **260**, C289–C296.
- ROME, L. C., SWANK, D. AND CORDA, D. (1993). How fish power swimming. *Science* **261**, 340–343.
- ROYET, J. P. (1991). Stereology: A method for analyzing images. *Prog. Neurobiol.* **37**, 433–474.
- SCHATTENBERG, P. J. (1973). Licht- und elektronenmikroskopische Untersuchungen über die Entstehung der Skelettmuskulatur von Fischen. *Z. Zellforsch. mikrosk. Anat.* **143**, 569–586.
- SHAPIRO, S. S. AND WILK, M. B. (1965). An analysis of variance test for normality (complete samples). *Biometrika* **52**, 591–611.
- SOKAL, R. R. AND ROHLF, F. J. (1981). *Biometry*, second edition. New York: W. H. Freeman and Company. 859pp.
- STREET, S. F. (1983). Lateral transmission of tension in frog myofibres: a myofibrillar network and transverse cytoskeletal connections are possible transmitters. *J. cell. Physiol.* **114**, 346–364.
- TIDBALL, J. G. (1983). The geometry of actin filament–membrane associations can modify adhesive strength of the myotendinous junction. *Cell Motil.* **3**, 439–447.
- TIDBALL, J. G. (1984). Myotendinous junctions: morphological changes and mechanical failure associated with muscle cell atrophy. *Exp. molec. Path.* **40**, 1–12.
- TIDBALL, J. G. AND CHAN, M. (1989). Adhesive strength of single muscle cells to basement membrane at myotendinous junctions. *J. appl. Physiol.* **67**, 1063–1069.
- TIDBALL, J. G. AND DANIEL, T. L. (1986). Myotendinous junctions of tonic muscle cells: Structure and loading. *Cell Tissue Res.* **245**, 315–322.
- TIDBALL, J. G. AND QUAN, D. M. (1992). Reduction in myotendinous junction surface area of rats subjected to 4-day spaceflight. *J. appl. Physiol.* **73**, 59–64.
- TROTTER, J. A. (1990). Interfiber tension transmission in series-fibered muscles of the cat hindlimb. *J. Morph.* **206**, 351–361.
- TROTTER, J. A. (1993). Functional morphology of force transmission in skeletal muscle: A brief review. *Acta anat.* **146**, 205–222.
- TROTTER, J. A. AND BACA, J. M. (1987). The muscle–tendon junctions of fast and slow fibres in the garter snake: Ultrastructural and stereological analysis and comparison with other species. *J. Muscle Res. Cell Motil.* **8**, 517–526.
- TROTTER, J. A., CORBETT, K. AND AVNER, B. P. (1981). Structure and function of the murine muscle–tendon junction. *Anat. Rec.* **201**, 293–302.
- TROTTER, J. A., EBERHARD, S. AND SAMORA, A. (1983a). Structural domains of the muscle–tendon junction. I. The internal lamina and the connecting domain. *Anat. Rec.* **207**, 573–591.
- TROTTER, J. A., EBERHARD, S. AND SAMORA, A. (1983b). Structural connections of the muscle–tendon junction. *Cell Motil.* **3**, 431–438.
- TROTTER, J. A., HSI, K., SAMORA, A. AND WOFSEY, C. (1985a). A morphometric analysis of the muscle–tendon junction. *Anat. Rec.* **213**, 213–226.
- TROTTER, J. A., SAMORA, A. AND BACA, J. M. (1985b). Three-dimensional structure of the murine muscle–tendon junction. *Anat. Rec.* **213**, 16–25.
- VAN LEEUWEN, J. L. (1995). Review article: The action of muscles in swimming fish. *Exp. Physiol.* **80**, 177–191.
- VAN LEEUWEN, J. L., LANKHEET, M. J. M., AKSTER, H. A. AND OSSE, J. W. M. (1990). Function of red axial muscles of carp (*Cyprinus carpio*) recruitment and normalized power output during swimming in different modes. *J. Zool., Lond.* **220**, 123–145.
- WANG, K., MCCARTER, R., WRIGHT, J., BEVERLY, J. AND RAMIREZ-MITCHELL, R. (1991). Regulation of skeletal muscle stiffness and elasticity by titin isoforms: a test of the segmental extension model of resting tension. *Proc. natn. Acad. Sci. U.S.A.* **88**, 7101–7105.
- WEIBEL, E. R. (1979). *Stereological Methods. Practical Methods for Biological Morphometry*, vol. 1, pp. 1–415. New York: Academic Press.
- WEIBEL, E. R. AND BOLENDER, R. P. (1973). Stereological techniques for electron microscopic morphometry. In *Principles and Techniques of Electron Microscopy. Biological Applications*, vol. 3 (ed. M. A. Hayat), pp. 237–297. New York: Van Nostrand Reinhold Company.